CHAPTER 25

EXPERIMENTAL STUDIES OF FORCES ON PILES

by

J. R. Morison, J.W. Johnson and M.P. O'Brien
Department of Engineering, University of California
Berkeley, Calif.

INTRODUCTION

In the design of a pile structure exposed to surface waves of a given height and period, some of the factors involved in the problem and studied herein are the size, shape and spacing of the piles and the moment distribution on uniform and non-uniform piles. Theoretical and experimental investigations have shown that the force exerted by surface waves on a pile consists of two components -- a drag force and an inertia force. The drag force is proportional to the fluid density, the projected area and the square of the fluid particle velocity. The inertia force, including the virtual mass, is proportional to the fluid density, the volume of the object and the fluid particle acceleration. The virtual mass is the apparent increase of the displaced mass of fluid necessary to account for the increase in force resulting from the acceleration of the fluid relative to the object. This factor is included in the coefficient of mass term in the force calculations.

The experimental and analytical approaches to the pile problem presented in this paper have been based on the total moment about the bottom of the pile and the moment distribution over the length of the pile. In order to calculate a theoretical moment it is necessary to obtain from the experimental results two empirical coefficients -- a drag coefficient and a mass coefficient (Morison, O'Brien, Johnson and Schaaf, 1950). The theoretical equations of total moment corresponding to the crest, trough, and still-water level positions along the surface wave are used to compute these coefficients from the measured total moments at the same positions. Using these coefficients and the theory, a comparison to experimental results is made by comparing the maximum moments, the phase relationships of maximum moments to the surface wave crest, and comparing the calculated and measured total moment time histories. A comparison of the coefficients obtained by these experiments to other published coefficients obtained in different manners, some being steady-flow values, shows that the results herein are of the right order of magnitude but have considerable variability.* Further investigation of the problems would clarify the reasons for the scatter of the coefficients.

Using the experimentally determined coefficients, the moment distributions on uniform diameter and variable diameter round piles were computed and compared to the measured distributions. The computed results are shown to predict the moment distribution with reasonable accuracy for design purposes.

* Errors occurred in Chapter 28, "Design of Piling" in the Proceedings, First Conference on Coastal Engineering and are corrected in the Appendix of this Chapter.

EXPERIMENTAL STUDIES OF FORCES ON PILES

The effects of size, shape and spacing of piles were obtained experimentally. Sheltering and mutual interference effects were found for piles arranged in rows or columns. Results are presented in comparative form as moment ratios with respect to a single cylindrical pile. Center piles in rows of piles aligned parallel to the wave crests showed maximum moments that were higher than those for a single isolated pile. The moment depended upon the relative clearances. Moments on piles arranged in columns parallel to the direction of the wave travel showed a sheltering effect on the center piles in the columns with moments less than those for a single isolated pile.

Moments on piles such as an H - section and a flat plate section were larger than those for cylindrical piles of the same projected area.

THEORETICAL CONSIDERATIONS

The dynamic force on an object in fluid moving with a steady-state velocity relative to the object is given by the expression

$$F = \frac{1}{2} C_D \rho A u^2 \qquad (1)$$

where

C_D = coefficient of drag.
ρ = fluid density.
A = projected area of object perpendicular to the velocity.
u = undisturbed fluid velocity relative to the object.

The coefficient of drag must be determined experimentally. It includes the dynamic effects of frictional drag and of form drag resulting from the disturbance of the fluid in the vicinity of the body.

In steady state fluid flow the drag coefficient is related to the flow by the Reynolds number given by the expression

$$R_e = \frac{Du}{\gamma} \qquad (2)$$

where

D = characteristic length of the object.
γ = kinematic viscosity of the fluid.

When the fluid is in non-steady motion past an object, the acceleration or deceleration of the fluid in the vicinity of the object produces a force component. Adding this force due to the fluid inertia to the frictional force, the total force is given by the expression (O'Brien and Morison, 1950),

$$F = \frac{1}{2} C_D \rho A u^2 + C_M \rho V_m \frac{du}{dt} \qquad (3)$$

where

C_M = coefficient of mass.
V_m = volume of the displaced fluid.
$\frac{du}{dt}$ = acceleration of the fluid relative to the object.

The coefficient of mass must be determined experimentally. This total force does not include any hydrostatic forces. The system under consideration is essentially in a balanced hydrostatic field.

A pile, extending vertically in a fluid in motion due to oscillatory waves, is in a non-uniform flow field with respect to time and to the submerged pile length. Consider a pile at any instant of time. Equation (3) must be written in the differential form and integrated over the pile length in order to obtain the total resultant force on the pile. In Equation (3) the area A is D dS and the displaced volume V_m is $(\pi D^2/4)$ dS. Thus, the differential force on the pile is given by the expression

$$dF = \left(\frac{1}{2} C_D \rho D u^2 + C_M \rho \frac{\pi D^2}{4} \frac{du}{dt}\right) dS \qquad (4)$$

where

D = pile diameter.
S = distance above the bottom into fluid.

Equation (4) may be integrated if C_D, C_M, and u, and du/dt are known as functions of time (t), or the phase angle, and of the position S. Taking S = (d + y + η) where d = depth of still water, y = depth below the mean water surface to the mean particle position (measured negatively downward), and η = vertical particle displacement about the mean position, and assuming that the horizontal particle velocity is zero when η = 0, then the horizontal velocity and acceleration of the fluid in wave action are given by the expressions (Stokes, 1901),

$$u = \frac{\pi H}{T} \frac{\text{Cosh } \frac{2\pi S}{L}}{\text{Sinh } \frac{2\pi d}{L}} \text{Cos } \theta \qquad (5)$$

and

$$\frac{du}{dt} = \frac{2\pi^2 H}{T^2} \frac{\text{Cosh } \frac{2\pi S}{L}}{\text{Sinh } \frac{2\pi d}{L}} \text{Sin } \theta \qquad (6)$$

where

H = wave height.
T = wave period.
L = wave length
θ = $2\pi t/T$, angular position of particle in its orbit measured counter-clockwise from the crest position at time t = 0.

The coefficients C_D and C_M depend upon the state of the fluid motion with respect to the object motion. Little is known about either of the coefficients in accelerated systems. As a first approximation they are considered as constant with respect to time and position to enable integration of Equation (4). Thus, C_D and C_M become overall coefficients.

This study is based on the total moment about the bottom of the pile, or the total moment contributed by the wave motion above any level, S_i, above the bottom. This moment is given by the expression

$$M_i = \int_{S_i}^{S_s} (S - S_i)\, dF \qquad (7)$$

In order to simplify the calculations of the first few experiments made, it was assumed that the wave elevation above or below mean water level contributed little to the total moment about the bottom; that is, η at the surface was small compared to d. Hence in Equation (7) the wave surface S_s is reduced to d and $S = d + y$. By making the necessary substitutions into Equations (4) and (7) and integrating, we have

$$F_i = \pi\rho \frac{D H^2 L}{T^2} \left\{ \pm C_D k_1 \cos^2\theta + C_M k_2 \frac{\pi D}{4H} \sin\theta \right\} \qquad (8)$$

$$M_i = \rho \frac{D H^2 L^2}{T^2} \left\{ C_D k_3 \cos^2\theta + C_M k_4 \frac{\pi D}{4H} \sin\theta - \frac{2\pi S_i}{L} \left[C_D \frac{k_1}{2} \cos^2\theta + \frac{k_2}{2} \frac{\pi D}{4H} \sin\theta \right] \right\} \qquad (9)$$

The line of action of the resultant total thrust, F_i, above the level, S_i is given by the expression

$$\bar{S} = \frac{M_i}{F_i} \qquad (10)$$

where

$$k_1 = \frac{\frac{4\pi d}{L} - \frac{4\pi S_i}{L} + \sinh\frac{4\pi d}{L} - \sinh\frac{4\pi S_i}{L}}{16 \left(\sinh\frac{2\pi d}{L} \right)^2} \qquad (11)$$

$$k_2 = \frac{\sinh\frac{2\pi d}{L} - \sinh\frac{2\pi S_i}{L}}{\sinh\frac{2\pi d}{L}} \qquad (12)$$

$$k_3 = \frac{\frac{1}{2}\left(\frac{4\pi d}{L}\right)^2 - \frac{1}{2}\left(\frac{4\pi S_i}{L}\right)^2 + \frac{4\pi d}{L}\sinh\frac{4\pi d}{L} - \frac{4\pi S_i}{L}\sinh\frac{4\pi S_i}{L} - \cosh\frac{4\pi d}{L} + \cosh\frac{4\pi S_i}{L}}{64 \left(\sinh\frac{2\pi d}{L} \right)^2} \qquad (13)$$

$$k_4 = \frac{\frac{2\pi d}{L}\sinh\frac{2\pi d}{L} - \frac{2\pi S_i}{L}\sinh\frac{2\pi S_i}{L} - \cosh\frac{2\pi d}{L} + \cosh\frac{2\pi S_i}{L}}{2\sinh\frac{2\pi d}{L}} \qquad (14)$$

Equation (9) for the total moment contains sine and cosine terms which are functions of the angular position, θ. Thus, a phase angle is indicated which depends upon the relative magnitude of the sine and cosine terms. The wave equations (5) and (6) are referenced at a wave crest at time $t = 0$. The phase angle, β, of the maximum moment in relationship to the wave crest is determined by differentiating Equation (9) with respect to θ and setting the results equal to zero; thus,

$$\beta = \sin^{-1}\left\{ \frac{\pi D C_M \left(k_4 - \frac{2\pi S_i}{L} \frac{k_2}{2} \right)}{8 H C_D \left(k_3 - \frac{2\pi S_i}{L} \frac{k_1}{2} \right)} \right\} \qquad (15)$$

The phase angle of Equation (15) shows that the maximum moment usually does not occur when a wave crest passes a pile. When the pile is in water which is shallow compared to the wave length (d/L small), the phase angle approaches zero. When the pile diameter is small compared to the wave height (D/H small) the phase angle also approaches zero. The phase angle approaches 90° for piles in deep water (d/L large) or for large piles in small waves (D/H large).

Measured moment-time histories on the pile and wave surface-time histories at the pile are used to determine C_D and C_M from Equation (9). Two variables are involved which necessitate selection of two times with the corresponding two moments. The solution is simplified if the selected times are zero (crest or trough at the pile) and the one-quarter or three-quarter wave length time (surface profile at the mean water level). These times result in $\sin\theta = 0$, and $\cos\theta = 0$, respectively. Thus, the selected points reduce Equation (9) to two equations, each with but one unknown, C_D and C_M, respectively.

The moment distribution on a non-uniform pile, that is a pile which consists of various lengths of different diameters (Fig. 1) results from a summation of the moments contributed by each section. The solution of Equation (9) for this system is given by the expression,

$$M_n = \sum_{j,i} \rho \frac{D_j H^2 L^2}{T^2} \left\{ C_D k_{3_i} \cos^2\theta + \frac{\pi D_j}{4H} C_M k_{4_i} \sin\theta - \frac{2\pi S_n}{L} \left[C_D \frac{k_{1_i}}{2} \cos^2\theta + \frac{\pi D_j}{4H} C_M \frac{k_{2_i}}{2} \sin\theta \right] \right\} \qquad (16)$$

where

$S_n = S_2, S_3, S_4, \cdots S_{11}$, the elevation at which the total moment is calculated.

$D_j = D_1, D_2, - - - D_5$, diameter of pile of various sections

k_{1_i} etc. $= k_{1_1}, k_{1_2}, - - k_{1_n}, k_{2_1}, k_{2_2} - - k_{2_n}$ the elevation above the bottom is being summed.

The conditions imposed upon Equation (16) in order to perform the summation resulting effect on Equations (11) to (14) are summarized for the conditions illustrated in Figure 1 as follows:

1. If $j = 1$ then $i = 2, 3$
   $j = 2$ $i = 4, 5$
   $j = 3$ $i = 6, 7$
   $j = 4$ $i = 8, 9$
   $j = 5$ $i = 10, 11$

2. For any $n = 2, - - -, 11$, the summation is carried out for successive values of j and the corresponding values of i until $i = n$. (See Fig. 1)

3. The expressions for k_{1i}, k_{2i}, k_{3i}, k_{4i} are the same as k_1, k_2, k_3, k_4 (Equations 11 to 14) where d in the numerator is changed to S_{i-1}. For example, Equation (11) becomes

$$k_{1i} = \frac{\frac{4\pi S_{i-1}}{L} - \frac{4\pi S_i}{L} + \text{Sinh}\frac{2\pi S_{i-1}}{L} - \text{Sinh}\frac{4\pi S_i}{L}}{16\left(\text{Sinh}\frac{2\pi d}{L}\right)^2}$$

The calculation of moments on piles in shallow water must include the effect of the variation of the lever arm between the crest and trough of the wave. The equation for the total moment about any level S_i is the same as Equation (9) where the expression of k_1, k_2, k_3, and k_4 (Equations 11, 12, 13 and 14) have S_s in the numerator instead of d. For example Equation (11) becomes

$$k_1 = \frac{\frac{4\pi S_s}{L} - \frac{4\pi S_i}{L} + \text{Sinh}\frac{4\pi S_s}{L} - \text{Sinh}\frac{4\pi S_i}{L}}{16\left(\text{Sinh}\frac{2\pi d}{L}\right)^2}$$

where S_s is the elevation to the water surface above the bottom.

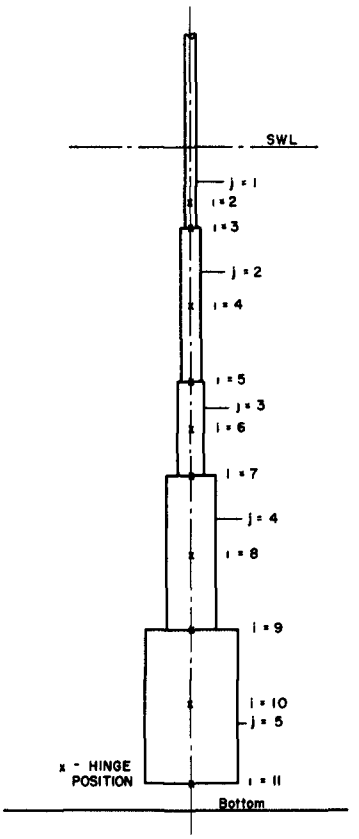

Fig. 1

The calculation of an explicit expression for the phase angle, similar to Equation (15) when considering the change in surface elevation is impossible so that it becomes necessary to plot a graph of equations or use approximate methods to obtain the phase angle of the total moment with respect to the wave crest (See Fig. 10).

In order to evaluate the total moment exerted on a pile subjected to a known wave condition, the coefficients C_D and C_M must be known. Measurements of the moment time history of piles subject to known wave conditions enable evaluation of C_D and C_M. The established coefficients then can be used to predict moments on piling for any pile and imposed wave conditions subject to the limitations and approximations of the analysis which leads to Equations (8), (9) and (15).

The drag coefficient, C_D, in Equations (8), (9) and (15) is comparable in significance to the steady state drag coefficient of Equation (1). Thus, comparisons may be made between the drag coefficients which result from measurements on piling subject to the periodic motion of wave action and those reported in the literature for the same geometrical systems in a steady state fluid stream. The steady state drag coefficients are functions of the Reynolds number, Equation (2), in addition to the

geometrical shape. In periodic motion the Reynolds No. varies from zero to a maximum. The maximum influence of the motion of a wave past a pile occurs near the surface in the regions of the highest velocity. Hence, the crest particle velocity is assumed to be most nearly representative of the velocity to be used in the Reynolds number. This results from Equation (5) with S = d and θ = 0.

EXPERIMENTAL INVESTIGATIONS ON MODEL PILES

Experiments were designed to measure the moment history on piles of constant and variable diameter about hinge points in the piles when subjected to wave action. The wave shape was measured simultaneously to determine the height, velocity, and period of the wave at the pile. The wave length is related to the velocity and period as follows:

$$L = C\,T \qquad (17)$$

From the measurements of the variables, the coefficients C_D and C_M were obtained from Equation (9). Once having determined the coefficient, then evaluation of the moments was possible for a given pile subjected to known wave action.

Experiments were conducted in the wave channel at the University of California (Morison, 1950a, 1950b, 1950c.

Tests on single circular piles: Moments were measured on single piles hinged at the bottom as well as at various elevations, (Fig. 2). In one instance a 1 inch diameter pile was hinged only at the bottom and subjected to a large range of wave conditions. In another series of tests, piles of 1/2, 1 and 2 inches in diameter were subjected to three different wave conditions, and the moments were obtained at hinge points located at various elevations to obtain moment distributions. A summary of test conditions is presented in Table 1, and a summary of the test results is given in Table 2.

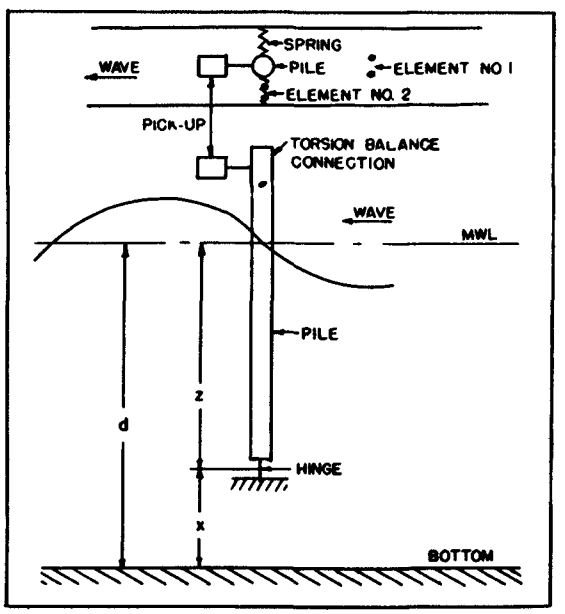

Fig. 2

Table 1.

Summary of test conditions on circular piles

Pile No.	D inches	d ft.	Wave Characteristics T-sec.	H-ft.	L-ft.	Remarks
1	1	2	(variable)			Moments measured only at the bottom
2	½	1.96	0.98	0.184	4.91	Moments measured at 7 elevations
3	1	1.96	0.98	0.179	4.98	Moments measured at 6 elevations
4	2	1.95	0.98	0.186	4.96	Moments measured at 6 elevations

Table 2.

Summary of test results on circular piles

Variable	Pile No. (See Table 1) 1	2	3	4
H/L	0.009 to 0.114	0.038	0.036	0.038
d/L	0.102 to 0.529	0.400	0.393	0.395
d/H	4.81 to 18.15	10.700	10.900	10.500
D/H	0.212 to 0.758	0.226	0.465	0.898
D/L	0.009 to 0.042	0.009	0.017	0.034
D/d	0.041 to 0.083	0.021	0.042	0.085
Re	2,000 to 11,100	2,300	4,500	9,300
C_D	1.6 ± 0.4	2.7	2.5	4.4 ($\beta = 80^o$)
C_M	1.5 ± 0.2	1.2	1.8	1.8

Some results were obtained for a pile placed in breaking waves. The departure of actual conditions from the assumed conditions as stated in the development of Equation (9) was too great to justify use of this equation in the interpretation of results in breakers. The results showed maximum moments produced by a breaker or incipient breaker greatly in excess of the forces corresponding to the orbital motion described by Equation (9)

The coefficients as determined for any one wave condition were used with Equation (9) to compute the complete moment history over the cycle from one wave crest to the next. A typical comparison is shown in Fig. 3.

Moment distribution comparisons were made for piles 2, 3, and 4 (Table 1). Equation (9), with values of C_D and C_M from the measured moment history at the bottom of the pile, was used to compute the moment ratio as a function of depth for comparison with the experimental ratio. Results are shown in Fig. 4.

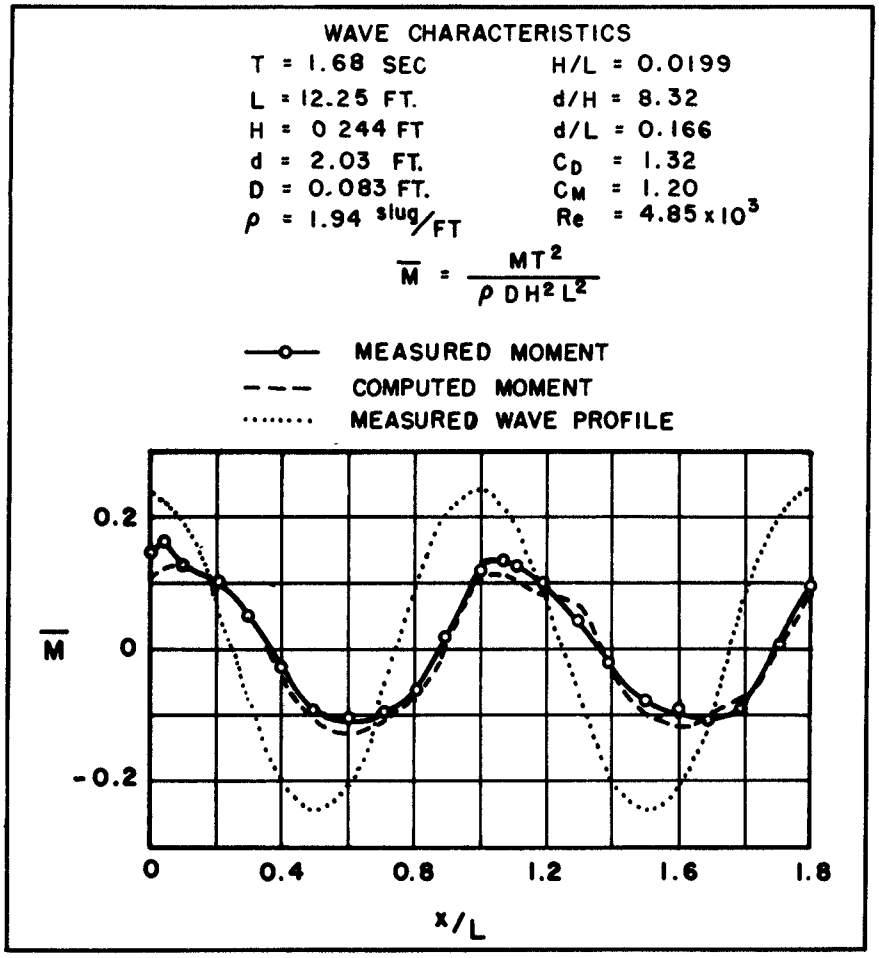

Fig. 3. Total moment about the bottom of a single circular pile.

In Fig. 4 certain features should be noted. The coefficients C_M and C_D were evaluated from the moment history at values of 0, $\pi/2$, π, $(3/2)\pi$ of the angular particle position with respect to the wave crest. Thus, the computed maximum moment may be different from the measured maximum moment for these conditions where the phase angle between the wave crest and maximum moment is different from zero. The computed curves, Fig. 3, show this difference. That is, at y/d = 1.00 (bottom), the maximum measured moment and the maximum computed moment do not coincide. However, the shape of the moment distribution as a function of depth, using the average values of C_D and C_M from the measured moment at the bottom to compute the moment at any depth, follows the trend of the measured moment distribution.

A further comparison may be made of the effect of pile diameter on the moment distribution by reducing the moment distribution to a ratio in terms of the maximum moments. Results are shown in Fig. 5 for one wave condition. The computed moment ratio and the experimental moment ratio are in agreement within the limits of experimental error. The pile diameter does not have any influence on the moment distribution. Hence, attention can be concentrated on obtaining moments about one hinge point to establish the necessary criteria to enable prediction of the moments on a pile due to wave action.

Within the accuracy of values of C_D and C_M, the resultant force as a function of time or wave position relative to the pile may be obtained from Equation (8). The action line of the total resultant force is obtained from

$$\bar{S} = \frac{M_d}{F}$$

where $\bar{S}$ is the location of the action line above the bottom and M_d is the moment about a hinge point at the bottom. The resultant force on a pile above a hinge point at any position in the pile may be obtained in a similar manner except for the section of the pile near the water surface.

In these tests forces were not computed, since attention was concentrated on obtaining reliable values of C_D and C_M from moment histories.

Tests on a variable diameter pile: The total moments exerted by waves on a pile which had varied steps of diameters was determined by a model study. The dimensions of the model are shown in Fig. 6. No attempt was made to determine the coefficients, C_D and C_M from the results on the stepped pile.

Three conditions of the stepped pile were investigated with respect to the coefficients C_D and C_M as determined in the discussions above for single cylindrical piles. The moment contributed for each section of the pile was computed from Equation (16) using $C_D = 1.63$, $C_M = 1.51$, and the experimentally measured phase angle, β_d, of the total moment about the bottom. Comparison of the moment distribution in the form of the ratio of the moment resulting from the wave action

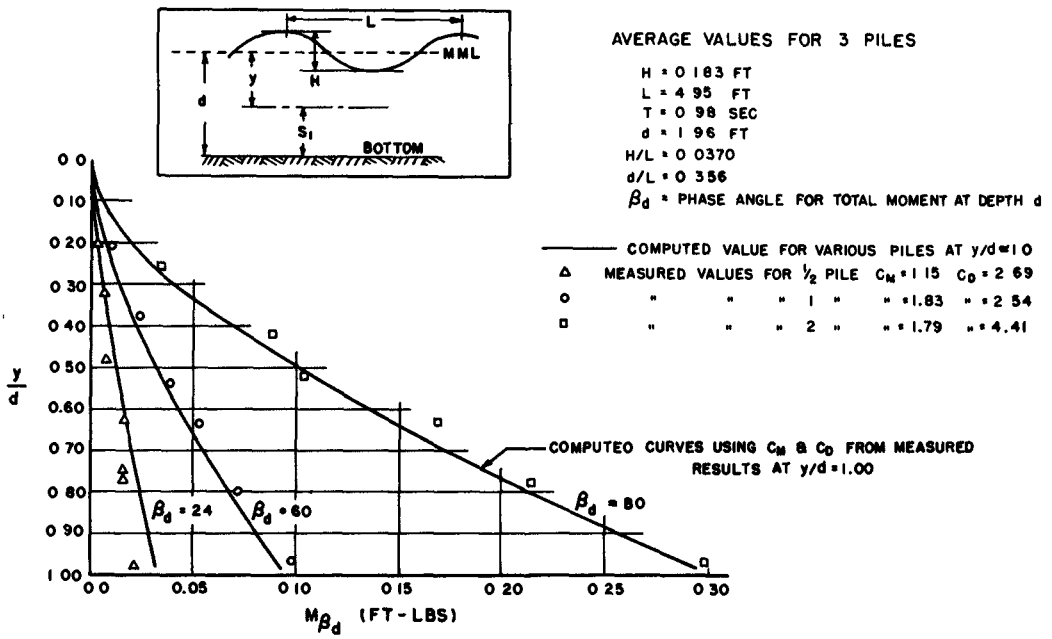

Fig. 4. Moment distribution on uniform pile - Laboratory results.

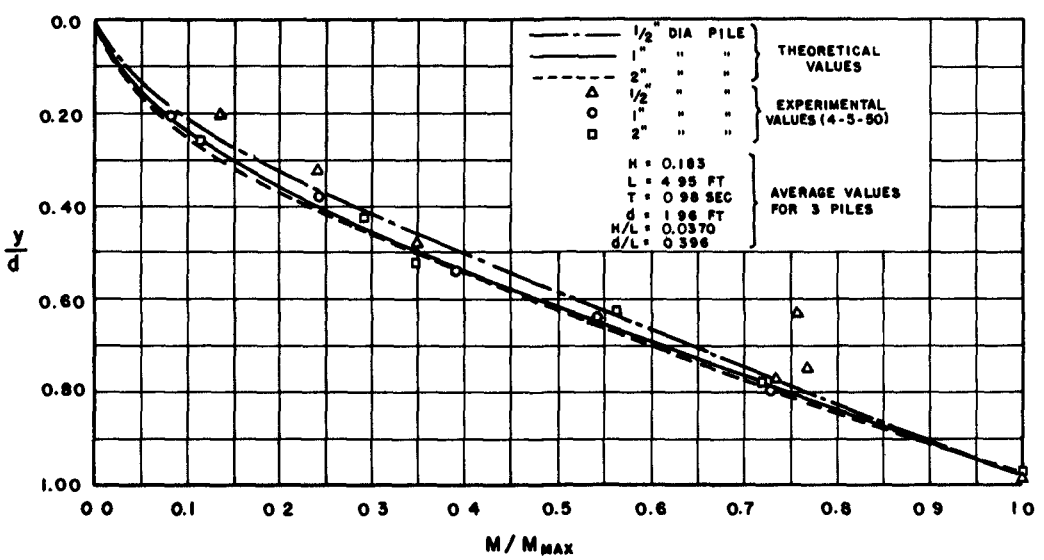

Fig. 5. Dimensionless moment distribution of uniform pile.

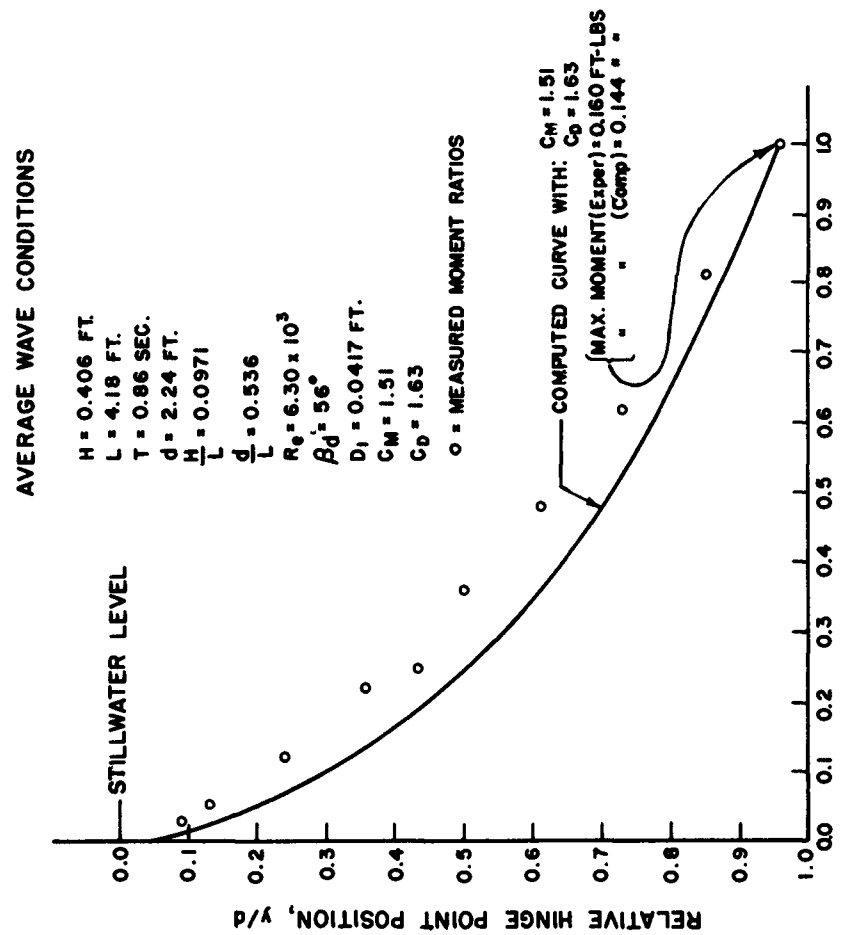

Fig. 7. Comparison of computed and measured moment distribution on a variable diameter pile.

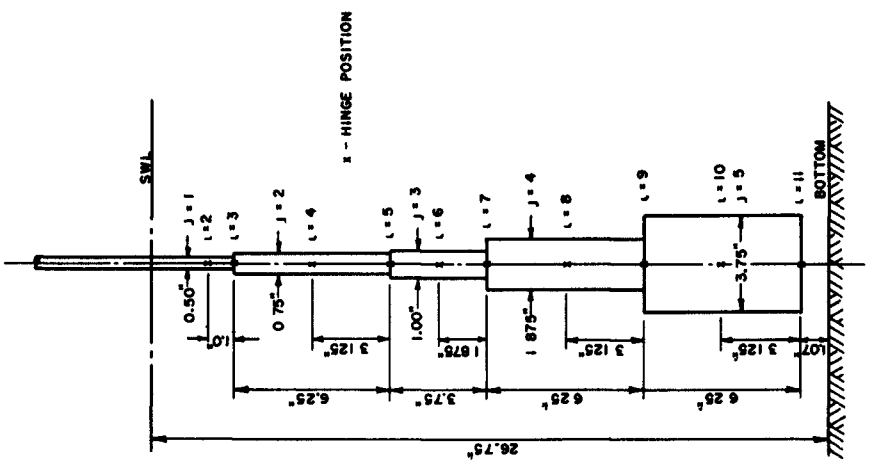

Fig. 6.

above any selected point to the maximum moment about the hinge point at the bottom is shown in Fig. 7.

Tests on piles of various cross-sectional shapes: The moment history of piles with various cross-sectional shapes was determined in the laboratory with the equipment shown in Fig. 1. The pile cross-sections were circular, flat plates and H - sections with one-inch projected width in the normal dimension as detailed in Fig. 8. Results were interpreted as ratios of the maximum moment for any given shape to the maximum moment for the circular shape (Table 4). The H - section was oriented in three different directions as shown in the table. All piles were subjected to the same wave conditions as indicated in Table 3.

Table 3

Wave conditions in tests on circular piles, flat plates and H - sections.

Parameter	Wave 1	Wave 2	Wave 3
H, ft.	0.681	0.342	0.454
L, ft.	7.54	3.87	5.39
T, sec.	1.27	0.88	1.09
d, ft.	1.55	1.50	0.83
H/L	0.0903	0.0884	0.0843
d/L	0.206	0.388	0.154

Table 4

Effect of pile shape on maximum moment.

Pile type and size	Orientation	Ratio: Maximum moment for given pile type / Maximum moment for circular pile		
1 inch round	→ ○	1.00 (β = 5°)	1.00 (β = 20°)	1.00 (Breaker) (β = 26°)
1 inch H-section	→ H α = 0	1.52 (β = 14°)	2.46 (β = 35°)	2.19 (β = 16°)
1 inch H-section	→ I α = 90°	1.42 (β = 10°)	2.08 (β = 43°)	2.58 (β = 41°)
1 inch H-section	→ H α = 45°	2.44 (β = 17°)	3.50 (β = 55°)	2.22 (β = 15°)
1 inch flat plate	→ |	1.28 (β = 4°)	1.17 (β = 37°)	1.37 (β = 9°)

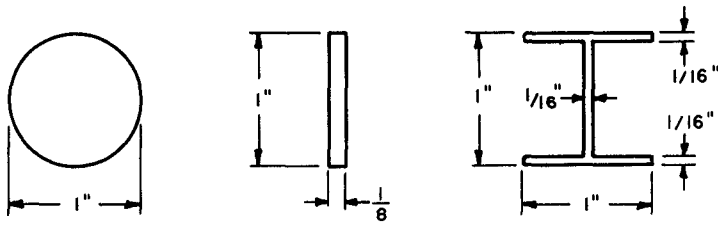

DIMENSIONS OF MODEL PILES

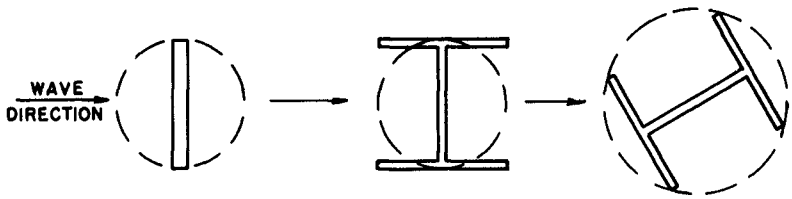

EQUIVALENT CYLINDER

SHOWN BY DASHED CIRCLE

Fig. 8. Cross sections of piles.

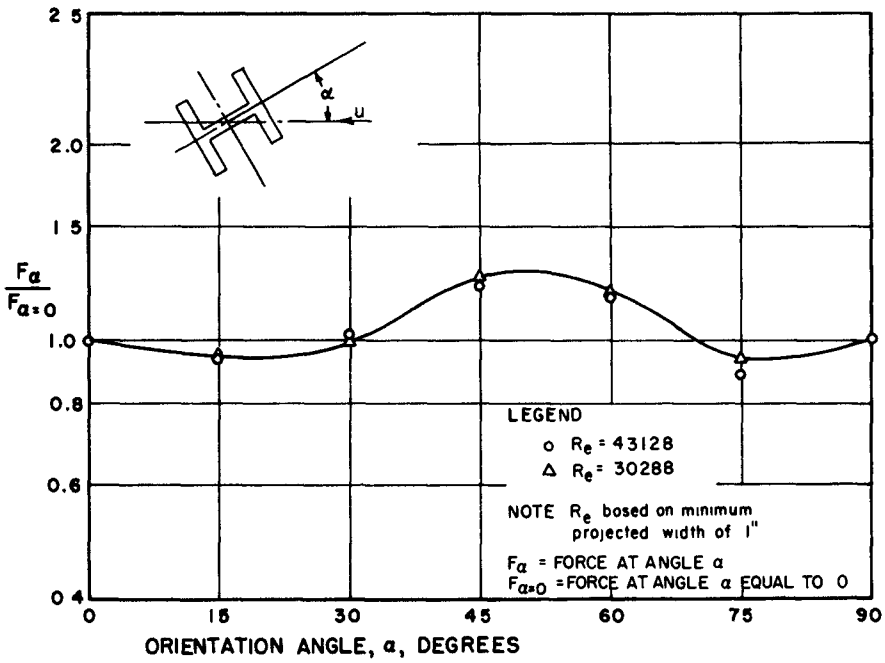

Fig. 9. Measured H-section drag force in steady, uniform flow as a function of orientation.

The force on the H - section was determined in a wind tunnel under steady-state condition as a function of orientation of the section. The maximum force resulted at approximately the 45° orientation as is shown in Fig. 9. Thus the pile results for that orientation were considered as giving the maximum moment (primarily because this orientation gave the greatest projected area); consequently, under wave action the orientation of the H-section was not varied over angles other than the 45° with respect to the direction of wave travel.

One comparison can be made using the H-section results of the steady-state force ratio and the maximum moment ratio in the wave action. Ratios of the maximum moment of the H-section oriented with values of α other than zero to the maximum moment with $\alpha = 0$ may be compared to the corresponding steady-state force ratios. (Note that the moment arm is constant in the comparison, hence moments should be in the same ratio as forces assuming the force distribution is similar and not a function of orientation.)

This comparison is shown in Table 5.

Table 5

Effect of orientation on forces on H-section in steady flow and in oscillatory flow.

Wave Steepness	Orientation of pile		
	→ H $\alpha = 0$	→ I $\alpha = 90°$	→ ⋋ $\alpha = 45°$
	Ratio: $\frac{\text{Force (or Moment) at orientation shown}}{\text{Force (or Moment) at } \alpha = 0}$		
0.0903	1.00	0.93	1.61
0.0884	1.00	0.85	1.42
0.0843 (Breaker)	1.00	1.17	1.02
Steady Flow	1.00	1.00	1.26

Differences between force ratios in steady state and in oscillatory flow are noted in some cases which are greater than any experimental error. Thus, the steady-state drag forces (hence steady-state drag coefficients) are not the complete criteria by which to evaluate moments of sections which differ from the circular section. This comparison would indicate the presence of the inertia force component, a fact which is confirmed by the differences in phase angles listed in Table 4.

The plots shown in Fig. 10 are computed, and measured moment-time histories of a circular, an H-section and a flat plate pile in shallow water where the effect of the variable lever arm has been considered by using S_s instead of d in Equations 11, 12, 13 and 14. The coefficients of drag and mass computed from the measured curve are given in Table 6 along with the wave characteristics.

Table 6

Coefficients of drag and mass for shallow water waves

Variable	Pile type		
	1 inch circular	1 inch H-section → H	1 inch flat plate → |
H, feet	0.613	0.600	0.705
L, feet	7.76	7.36	8.00
T, sec.	1.25	1.27	1.27
d, feet	1.50	1.46	1.45
H/L	0.079	0.082	0.088
d/L	0.193	0.198	0.181
β, degrees	5	14	0
R_e	15,000	15,000	15,000
C_D	1.78	2.44	1.20
C_M	0.44	1.92	0.42

One feature of the interpretation of the equations from which the coefficients of mass and drag were computed is evident in the results shown in Table 6. When the phase angle is small, the mass coefficient is evaluated from moments which are near the point of zero moment. Small experimental errors become significant and reduce the reliability of the value of the mass coefficient. The mass coefficients for the circular pile and the flat plate pile are small as compared to those reported in Table 2. These low coefficients are not representative.

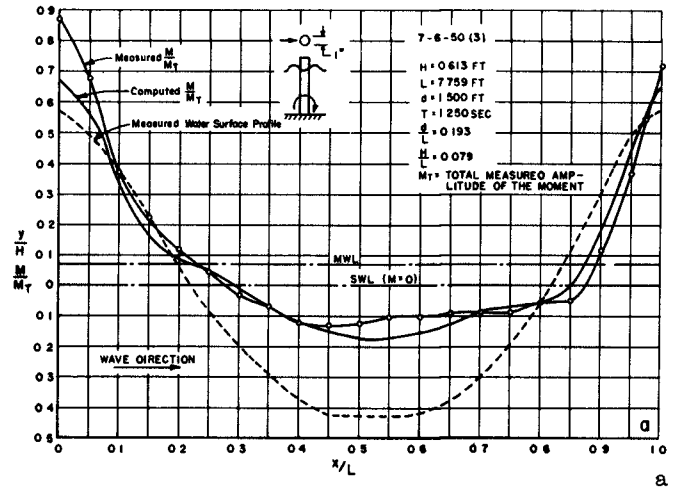

a

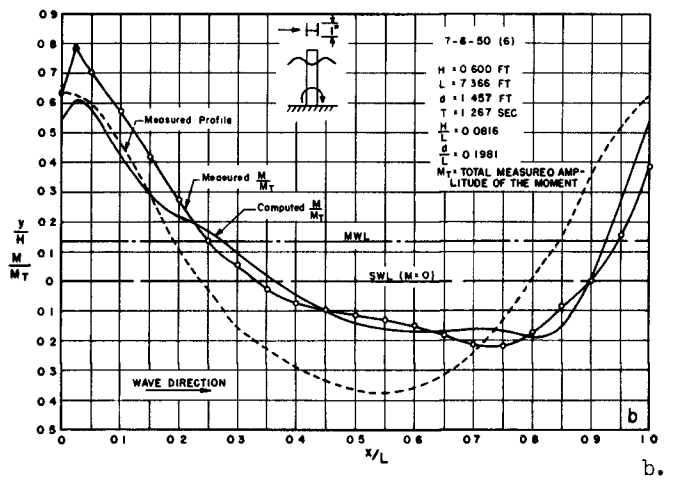

b.

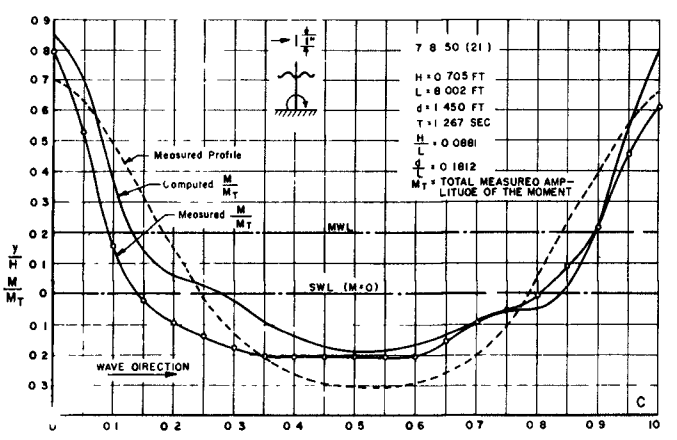

c.

Fig. 10. Computed and measured time history of total moment on circular, H-section, and flat plate piling.

Effect of mutual interference of piles: The one-inch circular and flat plate piles were arranged in rows parallel to the wave direction and in columns perpendicular to the wave direction (see Fig.11). Three piles were used in each case with moment measurements made on the center pile (Fig. 12). Spacings between the piles were ½D, D and 1½D, where D is the pile diameter. Results are shown in Table 7. The ratio of the maximum moment on the center pile of the column or row to the maximum moment on a single pile shows the results of interference effects. The wave conditions used were the same as listed in Table 3.

Table 7

Effect of mutual interference of piling

Wave Steepness, H/L (See Table 3)	Ratio: Moment on center pile / Moment on single pile		
	Pile Gap*		
	½ D	D	1½ D
	Row of circular pile perpendicular to wave travel		
0.0903	---	1.42	1.04
0.0884	2.43	0.90	0.94
0.0843 (Breaker)	1.69	1.14	1.23
	Row of flat plates perpendicular to wave travel		
0.0903	1.49	1.46	1.54
0.0884	1.93	1.40	1.17
0.0843 (Breaker)	2.22	1.72	1.31
	Column of circular pile parallel to wave travel		
0.0903	0.39	0.71	0.72
0.0884	0.60	0.71	0.74
0.0843 (Breaker)	0.96	0.76	0.87

* D = 1 inch for all piles.

The results show that, at spacings of less than 1½ D in the row arrangement, interference effects are noticeable. Higher moments are experienced by the center pile as contrasted to a single pile. The blocking effect of adjacent piles increases the force and resulting moment on an individual pile. The blocking effect decreases as the spacing between piles increases. For the limited range of the tests, the blocking effect is concluded to be negligible for spacings of 1½ D or greater.

Results from the piling arranged in columns show a sheltering effect, (Table 7,) in that moments were less than those represented by a

single pile. The maximum spacing at which the sheltering effect is negligible was not reached in these tests.

Forces on cross members: The measurement of the horizontal force on cross-members was made on a force balance apparatus. The cross-member was mounted on a rod which was pivoted near its center and restrained by calibrated springs at one end (Fig. 13). The submerged part of the rod was shielded from the wave action so that a tare test, without the cross-member attached, showed only about one-percent deflection. The force and the wave characteristics were recorded in the same manner as in the case of the single piles. Three lengths ($2\frac{1}{2}$, 5 and 10 inches) of cross-members were used so that the end effects could be determined.

The measurement of the vertical force on cross-members was made directly by a calibrated spring system. The cross-member was placed at the end of a vertical rod that was attached to springs (Fig. 14). The submerged part of the rod was shielded and held in guides near the cross-member. A tare test showed less than one-percent deflection. The wave characteristics were measured $1\frac{1}{2}$ feet in front and $1\frac{1}{2}$ feet behind the cross-member with a reference measurement of the wave crest being made directly above the cross-member. The force and wave characteristics were recorded simultaneously on the same oscillograph record. The same wave conditions were reproduced as those used for the measurement of the horizontal forces on the cross-members. In both the tests of the horizontal and of the vertical forces, the same wave conditions were used for the horizontal and inclined members at the 1/3 and 2/3 positions of water depth.

The horizontal force per unit length on a cross-member (Tables 8 and 9) indicated that the orientation of the cross-member is not critical for model studies. The test showed also that the end effects are not appreciable. The vertical force per unit length on a cross-member (Table 10) indicated some effects due to orientation. The magnitudes of the forces were about half those for the horizontal direction.

FIELD PILE TESTS

The model tests, as described above, yielded a considerable amount of information on the moments and forces on piles subjected to a wide range of wave conditions and depths of immersion. The limited size of the model system introduces a possible scale effect in the direct application of the model results to predict prototype behavior. Thus, prototype tests were made in an attempt to correlate model and prototype behavior to substantiate the analysis and results from the model tests (Snodgrass, Rice, and Hall, 1951).

The field tests were conducted near shore at Monterey, California, with a cylindrical pile of $3\frac{1}{2}$ inch outside diameter. The pile was hinged at the bottom at approximately sand level. Restraining bars at the top of the pile were arranged with strain gage elements connected to recording equipment. The strain records yielded the force-time history of the pile under the action of the incident waves. Calibrations of the strain recording equipment were made both in the laboratory and in the field.

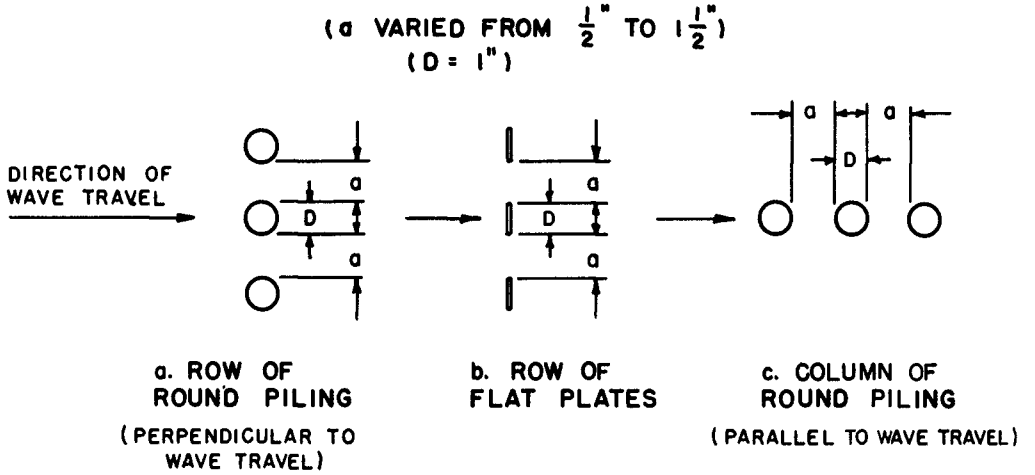

Fig. 11. Arrangement of piling for tests on mutual interference.

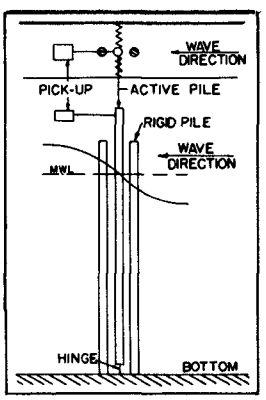

Fig. 12

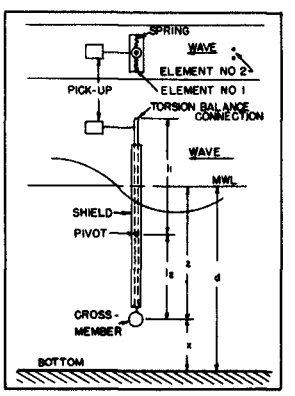

Fig. 13.

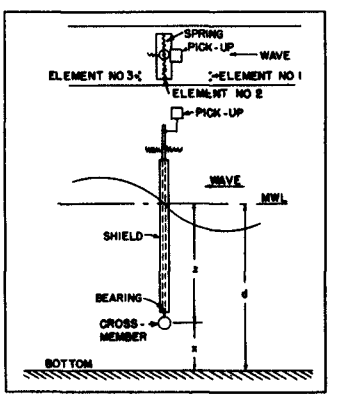

Fig. 14.

Table 8

Horizontal force on cross members.

Code	z ft.	d ft.	z/d	H ft.	L ft.	T sec.	F_{max} lbs.	F_{max} lbs/ft.	β_c deg.	d/L	H/L	C_{M90}	C_{M270}	C_{D_c}	C_{D_t}	R_e	I
8-15-50(14) 10 Hor.	1.054	1.543	0.683	0.615	6.172	1.200	0.05566	0.0868	56	0.250	0.0996	1.245	1.494	0.868	1.548		
8-15-50(17) 10 45 Cross	1.040	1.530	0.680	0.612	6.125	1.208	0.04465	0.0776	44	0.250	0.0999						
8-15-50(18) 10	1.054	1.543	0.683	0.622	6.084	1.200	0.06315	0.0638	84	0.254	0.1022						
8-15-50(19) 10	1.057	1.547	0.683	0.621	6.260	1.200	0.05818	0.0698	74	0.247	0.0992						
8-15-50(5) 5 Hor.	1.055	1.545	0.683	0.620	6.378	1.196	0.02345	0.0563	50	0.242	0.0972	1.103	1.163	0.776	1.505		
8-15-50(9) 5 45 Cross	1.050	1.540	0.682	0.602	6.172	1.200	0.02266	0.0544	53	0.250	0.0975						
8-15-50(10) 5	1.036	1.525	0.679	0.600	6.395	1.208	0.02328	0.0559	64	0.238	0.0938						
6-15-50(11) 5	1.052	1.543	0.682	0.606	6.172	1.200	0.02739	0.0657	90	0.250	0.0980						
6-15-50(25) 2½ Hor.	1.055	1.545	0.683	0.601	6.216	1.200	0.00858	0.0412	62	0.249	0.0967	0.892	1.486	0.588	1.852		
8-15-50(26) 2½ 45 Cross	1.039	1.528	0.680	0.605	6.172	1.200	0.00925	0.0444	60	0.248	0.0980						
6-15-50(28) 2½	1.039	1.528	0.680	0.636	6.353	1.200	0.01189	0.0571	60	0.241	0.1001						
8-15-50(27)2½	1.039	1.528	0.680	0.602	6.353	1.200	0.00925	0.0444	76	0.241	0.0948						
8-15-50(31) 10 Hor.	0.550	1.528	0.360	0.613	6.353	1.200	0.07008	0.0841	6	0.241	0.0965	0.618	0.847	0.633	1.061		
8-15-50(34) 10 45 Cross	0.570	1.549	0.368	0.612	6.172	1.200	0.08586	0.1030	6	0.251	0.0992						
8-15-50(35) 10	0.555	1.534	0.362	0.608	6.353	1.200	0.06186	0.0742	57	0.241	0.0957						
8-15-50(36) 10	0.570	1.550	0.368	0.620	6.171	1.200	0.09140	0.1097	86	0.251	0.1005						
8-15-50(39) 5 Hor.	0.570	1.550	0.368	0.618	6.259	1.183	0.04296	0.1031	30	0.248	0.0987	1.156	0.939	0.910	1.046		
8-15-50(42) 5 45 Cross	0.565	1.544	0.366	0.633	6.349	1.200	0.04160	0.0998	22	0.243	0.0997						
8-15-50(43) 5	0.560	1.539	0.364	0.600	6.548	1.183	0.03850	0.0924	46	0.235	0.0916						
8-15-50(44) 5	0.582	1.561	0.373	0.629	6.545	1.200	0.03550	0.0852	69	0.239	0.0961						
6-15-50(47) 2½ Hor.	0.545	1.524	0.358	0.630	6.548	1.183	0.01980	0.0950	45	0.233	0.0962	0.982	0.488	0.725	1.049		
6-15-50(50) 2½ 45 Cross	0.545	1.524	0.358	0.616	6.451	1.200	0.02980	0.1430	33	0.236	0.0955						
6-15-50(51) 2½	0.550	1.529	0.360	0.600	6.451	1.200	0.03480	0.1656	49	0.237	0.0930						
6-15-50(52) 2½	0.564	1.543	0.366	0.636	6.260	1.200	0.02540	0.1219	62	0.246	0.1016						
Average	1.047	1.538	0.681	0.614	6.306	1.198				0.244	0.0974					13,580	3.68
	0.561		0.365														

Table 9

Horizontal force on cross members.

Code		z ft.	d ft.	z/d	H ft.	L ft.	T sec.	F_{max} lbs.	F_{max} lbs/ft.	β_c deg.	d/L	H/L	$C_{M_{90}}$	$C_{M_{270}}$	C_{D_c}	C_{D_t}	R_e	I
8-16-50(8)	10" Hor.	0.518	1.503	0.345	0.324	3.204	0.783	0.03946	0.0474	53	0.469	0.1011	0.870	1.232	1.429	2.223		
8-18-50(9)	10" 45° Cross	0.519	1.503	0.345	0.340	3.204	0.783	0.03820	0.0458	44	0.469	0.1061						
8-16-50(10)	10"	0.514	1.499	0.343	0.337	3.204	0.783	0.04680	0.0562	90	0.468	0.1052						
8-16-50(11)	10"	0.507	1.492	0.340	0.327	3.241	0.783	0.05047	0.0606	90	0.460	0.1009						
8-16-50(14)	5" Hor.	0.500	1.485	0.337	0.331	3.167	0.775	0.01881	0.0451	53	0.469	0.1045	0.828	1.034	1.296	1.512		
8-16-50(17)	5" 45° Cross	0.500	1.485	0.337	0.317	3.314	0.792	0.02181	0.0523	61	0.448	0.0957						
8-16-50(18)	5"	0.501	1.485	0.337	0.317	3.314	0.792	0.02113	0.0507	77	0.448	0.0957						
8-18-50(18)	5"	0.504	1.489	0.338	0.317	3.276	0.792	0.02317	0.0556	90	0.455	0.0968						
8-18-50(22)	2½" Hor.	0.526	1.510	0.348	0.340	3.241	0.783	0.00788	0.0378	71	0.468	0.1049	0.818	0.680	0.846	1.550		
8-16-50(25)	2½" 45° Cross	0.512	1.496	0.342	0.330	3.207	0.775	0.01072	0.0515	72	0.466	0.1029						
8-16-50(28)	2½"	0.508	1.493	0.340	0.326	3.168	0.783	0.00946	0.0454	79	0.471	0.1029						
8-16-50(27)	2½"	0.500	1.485	0.337	0.339	3.204	0.783	0.01072	0.0515	90	0.463	0.1058						
8-16-50(30)	10" Hor.	1.000	1.493	0.670	0.350	3.277	0.783	0.01935	0.0232	90	0.456	0.1068	1.153	1.121	1.701	2.410		
8-16-50(32)	10" 45° Cross	0.998	1.493	0.668	0.343	3.275	0.790	0.02279	0.0273	90	0.456	0.1047						
8-16-50(33)	10"	1.001	1.496	0.669	0.334	3.178	0.750	0.01882	0.0223	83	0.471	0.1051						
8-18-50(34)	10"	1.001	1.496	0.668	0.334	3.278	0.783	0.01779	0.0213	90	0.457	0.1020						
8-16-50(37)	5" Hor.	0.991	1.486	0.867	0.305	3.204	0.783	0.00773	0.0126	88	0.464	0.0952	1.091	1.133	2.640	3.522		
8-16-50(40)	5" 45° Cross	0.999	1.494	0.669	0.350	3.069	0.750	0.00950	0.0228	83	0.487	0.1140						
8-18-50(41)	5"	0.992	1.487	0.667	0.337	3.205	0.783	0.00920	0.0221	83	0.464	0.1051						
8-16-50(42)	5"	0.999	1.494	0.669	0.350	3.133	0.783	0.00690	0.0166	90	0.477	0.1117						
8-18-50(45)	2½" Hor.	0.999	1.494	0.669	0.315	3.204	0.783	0.00205	0.0098	88	0.466	0.0983	0.568	0.649	0.834	1.669		
8-16-50(48)	2½" 45° Cross	1.004	1.499	0.670	0.312	3.209	0.767	0.00480	0.0230	80	0.467	0.0972						
8-16-50(49)	2½"	0.987	1.482	0.666	0.323	3.139	0.767	0.00440	0.0211	90	0.472	0.1029						
8-16-50(50)	2½"	0.994	1.489	0.668	0.326	3.139	0.767	0.00560	0.0269	88	0.474	0.1039						
Average		0.509	1.493	0.341	0.330	3.211	0.779				0.465	0.1028					10,290	1.98
		0.997		0.668														

Table 10

Vertical force on cross members

Code	z ft.	d ft.	z/d	H ft.	L ft.	T sec.	F_{max} lbs.	F_m lbs/ft.	β_c deg.	d/L	H/L	C_{M_o}	C_{M_t}	$C_{D_{90}}$	$C_{D_{270}}$	R_e	I
9-7-50(3) 5 Hor.	1.063	1.537	0.692	0.568	6.452	1.183	0.01567	0.0376	70	0.238	0.0880	0.467	1.649	3.954	3.051		
9-7-50(6) 5 45° Cross	1.010	1.484	0.681	0.521	7.002	1.167	0.01095	0.0262	66	0.212	0.0744						
9-7-50(8)	1.045	1.519	0.688	0.520	6.357	1.183	0.01518	0.0364	118	0.239	0.0818						
9-7-50(7)	1.072	1.546	0.693	0.545	6.360	1.200	0.02125	0.0510	110	0.243	0.0857						
9-7-50(11) 5 Hor.	0.537	1.527	0.352	0.540	6.452	1.183	0.03063	0.0733	98	0.237	0.0837	0.0686	1.309	1.425	0.969		
9-7-50(14) 5 45° Cross	0.524	1.514	0.342	0.509	6.878	1.183	0.02856	0.0686	70	0.219	0.0740						
9-7-50(16) 5	0.547	1.537	0.356	0.525	6.755	1.200	0.03116	0.0748	104	0.228	0.0777						
9-7-50(15) 5	0.539	1.529	0.353	0.559	5.652	1.183	0.03765	0.0904	98	0.230	0.0840						
Average	1.048	1.524	0.688	0.536	6.614	1.185				0.230	0.0810					12,210	3.22
	0.537		0.352														
9-7-50(20) 5 Hor.	0.564	1.554	0.363	0.325	3.138	0.758	0.02133	0.0512	110	0.495	0.1036	1.554	0.225	1.903	4.469		
9-7-50(24) 5 45° Cross	0.509	1.499	0.340	0.322	3.247	0.767	0.01476	0.0354	107	0.462	0.0992						
9-7-50(23)	0.509	1.499	0.340	0.306	3.102	0.758	0.02276	0.0546	124	0.483	0.0986						
9-7-50(25)	0.499	1.489	0.335	0.310	3.209	0.767	0.02860	0.0686	130	0.464	0.0966						
Average	0.520	1.510	0.344	0.316	3.174	0.763				0.476	0.0996					10,050	1.90

The wave height history was obtained from a recording pressure actuated diaphragm type wave meter which was located approximately two feet above the sand bottom and adjacent to the pile. Two auxiliary graduated piles were placed seaward of the measuring pile. The measuring pile and bracing structure also were painted with alternate black and white bands, each one foot high. Motion pictures taken from the beach recorded the surface profile of the waves as they passed the pile. A clock was suspended in the field of view of the camera to provide timing intervals between successive frames of the film. The wave velocity at the pile was obtained from the distance between the seaward auxiliary pile and the measuring pile (19.8 feet), and the time interval of the wave crest travel between these points. The motion pictures also recorded wave heights at the measuring pile. Trough and crest elevations of each wave were obtained from the intersection of the water profile with the graduated vertical piles. The record from the wave meter also gave wave heights and periods.

Analysis of data: The analysis as presented previously in this paper includes the two resistance terms that contain C_D and C_M, and also the phase angle relationship, β, between the two resistance terms. In the analysis of the field pile results, the timing accuracy was not precise enough to determine the time comparison between the water surface profile and the moment history.

The data and results were obtained for waves in various conditions depending on the stage of the tide. Some data were obtained with the pile in a foam line shoreward of the breaker. Other data were obtained with the pile in the smooth unbroken swell seaward of the breaker. The data have been segregated with respect to the wave condition at the pile into the following groups: (1) foam line; (2) foam line immediately shoreward of the breaker point; (3) breaker; (4) sharp peaked swell at incipient break; (5) sharp peaked swell immediately seaward of the breaker point; and (6) swell some distance seaward of the breaker point. The data are summarized in Table 11.

The wave force, which is actually a distributed force extending from the ocean bottom to the water surface, was recorded as an equivalent force at the calibration point. By multiplying the recorded force by the calibration-point lever-arm (9 feet 8 inches) the total moment of the wave force about the bottom hinge was determined. When the maximum force exists (approximately at the time the wave crest passes the pile), the centroid of the wave force was assumed to be located near the mean height of the wave. This location of the centroid was estimated by considering the horizontal component of the particle motion as observed in model studies. By computing the wave force at the mean wave height, as defined above, the data were found to be reasonably consistent. The values obtained from the computation indicate that waves of a given size and shape will exert the same force at the centroid independent of water-level changes over the range encountered in the tests, although the moment about the hinge point varied considerably due to variation of the effective lever arm as the water depth changed. A graph of the wave force at mean wave height is shown in Fig. 15.

Table 11
Test data on field pile

WAVE NO.	WAVE TYPE*	WAVE HEIGHT H Ft.	WAVE PERIOD T Sec.	WAVE VELOCITY (MEASURED) C_c Ft./Sec.	ELEVATION OF CREST ON PILE S_c Ft.	ELEVATION OF TROUGH ON PILE S_t Ft.	STILL WATER LEVEL $d = S_t + \frac{H}{3}$ Ft.	OBSERVED FORCE F_r Lbs.	TOTAL MOMENT M Ft-Lbs.	COEFFICIENT OF DRAG C_D
1	FL	4.6	10.7	---	8.0	3.4	5.20	87	562	-
2	FL	4.5	12.1	18.8	8.0	3.5	5.00	57	552	1.05
3	FL	4.2	11.7	17.8	8.0	3.8	4.83	64	525	1.71
4	FL	4.2	9.3	17.5	7.5	3.4	4.20	64	629	1.34
5	FL	4.0	8.3	19.5	7.4	3.4	4.73	34	330	0.63
6	FL	3.8	12.0	17.5	7.0	3.4	4.93	51	496	1.59
7	FL	3.6	7.7	15.8	5.8	2.2	3.40	53	515	1.52
8	FL	3.5	10.3	15.7	6.9	3.4	4.57	33	320	1.46
9	FL-B	4.1	12.1	18.7	7.4	3.3	4.67	48	475	1.91
10	B-FL	4.8	8.3	20.1	8.5	3.7	5.10	51	496	1.59
11	B	5.0	10.1	21.8	8.2	3.2	4.87	55	535	0.49
12	B	4.8	12.2	23.5	8.3	3.5	4.60	57	552	0.63
13	B	3.9	11.2	14.9	5.7	2.8	4.20	32	310	1.05
14	B	3.8	10.5	18.7	7.0	3.1	4.40	27	265	0.73
15	B	3.8	8.4	17.9	6.4	2.8	4.00	34	330	0.91
16	B	3.3	11.0	14.4	5.2	1.9	3.00	28	279	1.31
17	B	3.3	10.3	14.2	5.7	3.4	4.50	23	225	1.28
18	B	3.0	-----	-----	5.5	3.5	4.50	23	226	-
19	SP-B	3.4	11.0	14.8	5.8	2.4	3.53	17	165	0.85
20	SP-B	3.3	10.8	15.5	7.0	3.7	4.80	19	185	0.88
21	SP-B	3.3	9.0	14.4	6.0	2.7	3.80	13	124	0.64
22	SP-B	2.3	13.1	14.3	5.0	2.7	3.47	3	33	0.39
23	SP-B	2.0	8.5	15.9	4.8	2.8	3.47	4	43	0.57
24	SP	4.5	----	---	7.8	3.5	4.80	5	46	-
25	SP	3.7	---	---	5.2	2.5	3.73	12	113	-
26	SP	3.8	12.1	18.8	7.4	3.8	4.80	17	166	0.44
27	SP	3.5	12.1	20.1	5.9	3.4	4.57	11	109	0.28
28	SP	3.3	10.8	14.8	8.0	2.7	3.70	14	134	0.64
29	SP	3.5	9.1	14.8	5.8	3.3	3.70	8	82	0.26
30	SP	3.1	13.0	17.7	6.8	3.7	4.75	18	175	0.78
31	SP	3.1	10.0	14.2	5.8	2.8	3.83	10	93	0.49
32	SP	3.0	11.0	15.5	6.5	3.6	4.87	9	88	0.46
33	SP	2.9	10.3	13.0	5.4	2.5	3.47	8	75	0.60
34	SP	2.8	11.7	14.8	8.1	3.3	4.23	8	83	0.68
35	SP	2.7	----	---	5.0	3.3	4.20	5	53	-
36	SP	2.6	----	----	5.9	3.3	4.50	5	51	-
37	S	3.4	9.3	15.7	5.7	3.3	4.43	9	85	0.32
38	S	3.3	9.4	12.5	5.2	2.9	4.00	15	155	0.98
39	S	3.0	8.4	18.8	5.4	3.4	4.40	12	130	0.59
40	S	2.9	4.5	16.7	5.5	3.8	4.57	5	58	0.27
41	S	2.7	9.3	14.1	5.4	3.7	5.00	8	57	0.53
42	S	2.7	7.5	15.1	5.9	3.2	4.10	7	70	0.54
43	S	2.5	9.4	13.5	5.9	3.3	4.17	7	72	0.80
44	S	2.5	----	----	5.9	3.4	4.23	7	70	-
45	S	2.4	11.8	16.6	5.7	3.3	4.10	3	33	0.29
46	S	2.4	10.7	18.8	5.0	2.6	3.40	8	75	0.57
47	S	2.4	8.5	16.6	6.0	3.6	4.40	8	52	0.57
48	S	2.4	8.2	15.8	5.6	3.2	4.00	5	45	0.43
49	S	2.3	11.8	18.4	6.7	4.4	5.07	11	108	0.86
50	S	2.3	6.8	---	5.7	3.4	4.17	3	28	-
51	S	2.2	8.4	---	6.9	3.7	4.43	4	41	-
52	S	2.2	8.8	15.7	5.2	3.0	3.73	6	50	0.74
53	S	2.1	13.1	----	6.5	3.4	4.10	6	56	-
54	S	2.1	7.7	13.8	4.9	2.8	3.50	2	15	0.25
55	S	2.1	7.5	14.1	5.2	4.1	4.67	4	35	0.63
56	S	2.1	7.0	21.4	5.3	3.2	3.90	4	38	0.29
57	S	2.1	----	----	6.5	4.4	5.10	8	74	-
58	S	2.0	11.4	12.5	4.8	2.8	3.55	3	28	0.66
59	S	2.0	7.5	19.1	5.2	3.2	3.87	6	54	0.58
60	S	2.0	5.0	14.4	5.5	3.5	4.17	5	47	0.86
61	S	2.0	4.4	18.8	5.2	4.2	4.87	6	62	0.88
62	S	2.0	---	---	5.2	3.2	3.87	4	35	-
63	S	1.8	10.0	14.8	5.8	3.9	4.43	2	21	0.45
64	S	1.9	----	---	6.4	4.5	5.13	5	41	-
65	S	1.8	12.4	21.4	5.2	3.4	4.00	4	23	0.24
66	S	1.8	10.0	11.0	4.5	2.7	3.30	3	25	0.94
67	S	1.8	8.8	21.7	8.0	4.2	4.80	6	79	0.88
68	S	1.8	9.1	20.2	5.7	3.9	4.50	4	35	0.43
69	S	1.7	11.5	22.4	8.2	4.5	5.07	7	68	0.88
70	S	1.7	10.3	---	6.4	4.7	5.27	5	47	-
71	S	1.7	---	---	4.4	2.7	3.27	2	17	-
72	S	1.7	---	---	5.4	3.7	4.27	4	33	-
73	S	1.8	11.1	---	4.2	2.6	3.13	1	4	-
74	S	1.6	10.8	14.6	4.8	3.2	3.73	2	17	0.54

* FL (Foam line); B (Breaker); SP-B (Sharp peak swell starting to break); FL-B (Breaker with some foam); SP (Sharp peak swell); S (Swell).

EXPERIMENTAL STUDIES OF FORCES ON PILES

Table 11 cont'd.

Test data on field pile

WAVE NO.	WAVE TYPE	WAVE HEIGHT H Ft.	WAVE PERIOD T Sec.	WAVE VELOCITY (MEASURED) C_p Ft./Sec.	ELEVATION OF CREST ON PILE S_c Ft.	ELEVATION OF TROUGH ON PILE S_t Ft.	STILL WATER LEVEL d $S_t \frac{H}{C}$ Ft.	MEASURED FORCE F Lbs.	TOTAL MOMENT M Ft-Lbs.	COEFFICIENT OF DRAG C_D
75	S	1.6	8.8	-----	5.2	3.6	4.13	3	30	-----
76	S	1.6	7.8	14.9	5.3	3.7	4.23	3	33	0.96
77	S	1.8	4.2	-----	5.5	3.9	4.43	3	27	-----
78	S	1.6	-----	-----	5.4	3.8	4.33	3	33	-----
79	S	1.5	10.6	16.7	5.3	3.8	4.30	2	19	0.52
80	S	1.5	9.0	-----	5.0	3.5	4.00	1	5	-----
81	S	1.5	8.3	17.3	4.4	2.9	3.40	1	14	0.37
82	S	1.5	-----	-----	5.1	3.6	4.10	3	33	-----
83	S	1.4	12.2	19.2	4.2	2.8	3.27	3	29	0.63
84	S	1.4	10.0	-----	5.8	4.4	4.60	2	21	-----
85	S	1.4	-----	-----	5.4	4.0	4.47	4	37	-----
86	S	1.4	-----	-----	5.9	4.5	4.97	3	34	-----
87	S	1.3	10.2	-----	4.7	3.4	3.83		29	-----
88	S	1.3	5.8	-----	5.5	4.2	4.63	2	17	-----
89	S	1.3	-----	-----	6.0	4.7	5.13	3	29	-----
90	S	1.3	-----	-----	6.0	4.7	5.13	5	48	-----
91	S	1.3	-----	-----	5.8	4.5	4.73	4	37	-----
92	S	1.3	-----	-----	5.0	3.7	4.13	3	29	-----
93	S	1.2	13.3	-----	4.8	3.4	3.80	2	21	-----
94	S	1.2	12.4	12.3	5.8	4.8	5.00	3	29	2.72
95	S	1.2	11.4	15.1	4.9	3.7	4.10	2	19	1.14
96	S	1.2	10.3	10.4	6.0	4.8	5.17	3	34	-----
97	S	1.2	-----	-----	4.7	3.5	3.93	2	22	-----
98	S	1.1	11.8	12.5	3.9	2.8	3.17	1	12	1.06
99	S	1.0	12.7	-----	4.7	3.7	4.03	1	10	-----
100	S	1.0	12.2	13.7	3.7	2.7	3.03	2	17	1.60
101	S	1.0	-----	-----	4.3	3.5	3.83	1	10	-----
102	S	0.9	9.8	18.5	3.8	2.7	3.00	1	8	1.23
103	S	0.8	6.8	-----	3.2	4.4	4.53	1	13	-----
104	S	0.8	-----	-----	3.4	4.8	4.87	1	12	-----
105	S	0.7	-----	-----	4.9	4.2	4.43	1	10	-----
106	S	0.7	-----	-----	4.8	3.9	4.13	1	8	-----
107	S	0.6	7.1	19.8	5.0	4.4	4.60	2	18	2.38

* S (Swell).

One feature becomes apparent in reviewing the data that permits a comparison between the model results and the field test results. The majority of the field test conditions were obtained with samll ratios of the pile diameter to the wave height, and with small ratios of the water depth at the pile to the wave length. Under these conditions, the phase angle as given by Equation (15) approaches zero and the maximum moment of Equation (9) occurs when the time angle, θ, is zero.

Equation (9) for a pile hinged at the bottom then reduces to

$$M_{max} = \rho \frac{D H^2 L^2}{T^2} C_D k_3' \tag{18}$$

k_3' is introduced as a refinement of k_3 to include an approximation of velocity distributions in a wave of finite height in shallow water; that is,

$$k_3' = \frac{\frac{1}{8}\left(\frac{4\pi S_c}{L}\right)^2 + \frac{4\pi S_c}{L}\operatorname{Sinh}\frac{4\pi S_c}{L} - \operatorname{Cosh}\frac{4\pi S_c}{L} + 1}{64\left(\operatorname{Sinh}\frac{2\pi d}{L}\right)^2} \tag{19}$$

where $d = S_t + 1/3\ H$ (assumed still-water level)
S_c = wave crest elevation above the bottom
S_t = wave trough elevation above the bottom
H = wave height

For small values of d/L, Sinh $4\pi S_c L$ is approximated by $4\pi S_c/L$, and Sinh $2\pi d/L$ is approximated by $2\pi d/L$. These approximations result in

$$k_3' = \frac{3}{32}\frac{S_c}{d} \tag{20}$$

and

$$C_D = \frac{32}{3}\frac{M_{max} T^2 d}{\rho D H^2 L^2 S_c} \tag{21}$$

As the wave velocity is related to the length and period by $C = L/T$, we find that

$$C_D = \frac{32}{3}\frac{M_{max} C^2 d}{\rho D H^2 S_c} \tag{22}$$

All variables on the right side of Equation (22) were measured and C_D then computed. C_D is a drag coefficient which depends upon the state of the disturbance of the wave motion due to the movement of the wave past the pile. For shallow-water waves, the velocity distribution from the crest of the wave to the bottom is a function of the ratio of wave height to water depth, and is essentially independent of the wave length or period. The resulting moment on the pile, and hence C_D, are functions of this ratio, H/d. The results are shown in Fig. 16 on this basis, with segregation of the results according to wave type. The field pile results were obtained for wave conditions of d/L less than 0.06, with the majority of the waves characterized by d/L less than 0.03.

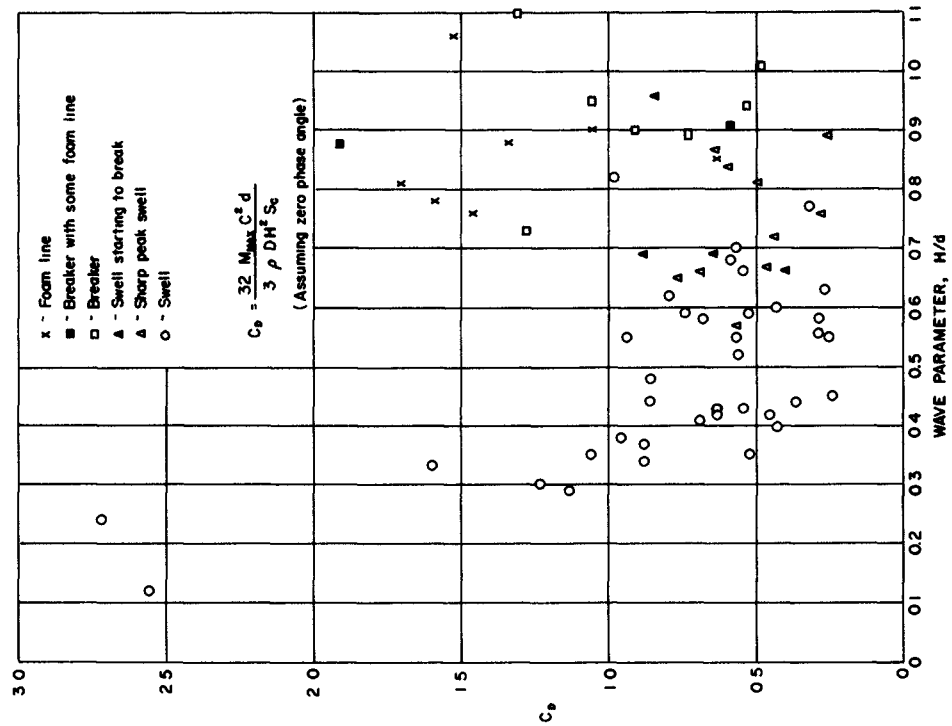

Fig. 16. Coefficient of drag computed from field tests on a circular pile.

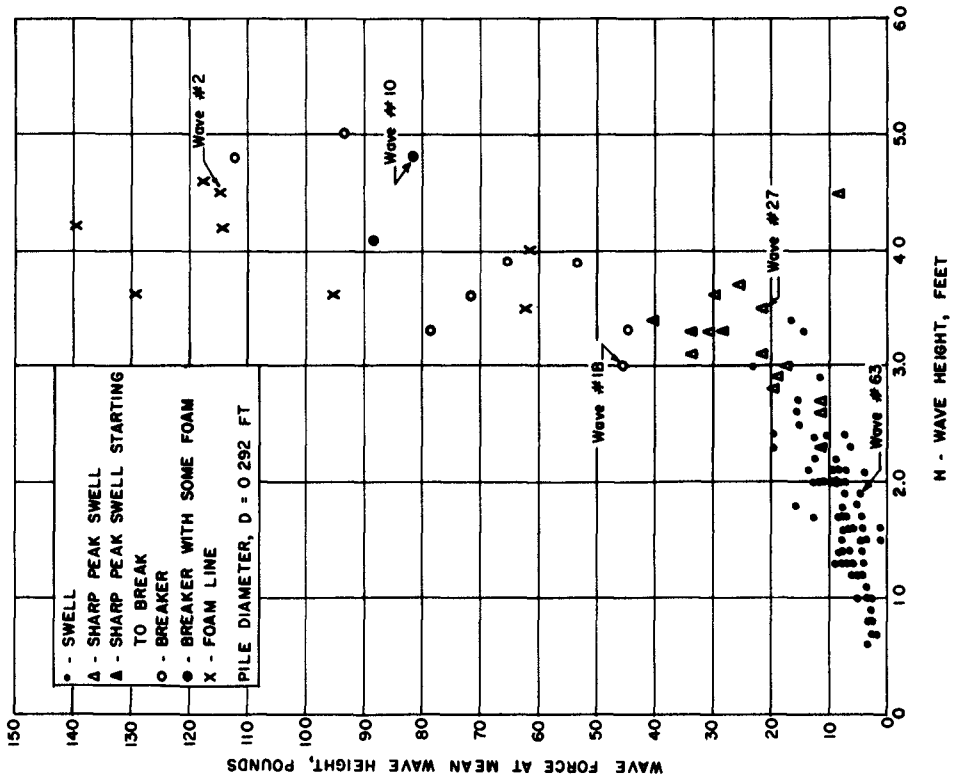

Fig. 15. Wave force at mean wave height as a function of wave height.

The scatter of the results reflects the accuracy of the data and the accuracy of the assumptions of Equation (22), C_D is computed from Equation (22) which contains the square of the wave velocity and the square of the wave height. Small discrepancies of these variables may produce appreciable differences in C_D. The maximum moment was obtained from the force, which was measured to within one pound. Many of the measured forces were from one to five pounds. Some scatter of results is necessarily expected.

Enough data were taken to permit the following general observations.

1) Foam lines and breakers produce higher values of C_D than unbroken swells.

2) For values of H/d greater than 0.4, an average value of C_D equal to 0.50 best represents the results.

3) For values of H/d less than 0.4, C_D becomes larger than 0.50. The assumptions of Equation (22) become invalid in this range of H/d.

A direct comparison of the model test results with the field test results cannot be made. The same range of the governing parameters was not covered in the two series of tests, particularly the ranges of d/L and H/d. In Fig. 16 drag coefficients of 1.0 to 2.5 are shown for values H/d between 0.4 and 0.1. These magnitudes of the drag coefficients are in the same range as those obtained from the model studies. However, the values of d/L of the field tests were not the same as the model tests. As mentioned in the model test summary, complete correlations including all defining parameters have not yet been attained. No attempts have been made to carry the field results beyond Fig. 16.

CONCLUSIONS

The analysis of forces and moments on piles as summarized herein contains two coefficients which must be determined experimentally: the coefficient of mass and the coefficient of drag. The results so far obtained indicate that the theoretical value of 2.0 for the coefficient of mass is adequate for computing the forces on circular piling. For the coefficient of drag, however, additional results are needed with a large range of the variables of pile diameter, wave height, wave length, and water depth.

The results show that moments measured about a single hinge point will suffice in establishing the magnitudes of the coefficients. The moment distribution from coefficients obtained from moments about a bottom hinge point agree with measured moment distributions.

Measured moments on piles of cross-sectional shape other than circular show coefficients which are a function of the shape of the pile. Steady-state drag coefficients can not be used as drag coefficients in the analysis of periodic motion.

Results of the interference effects of rows of circular piling, while limited in scope, indicated that for clearances greater than 1½ pile diameters the interference effects are negligible. Moments on center piles of a row are increased as compared to moments on an isolated pile for spacings less than 1½ pile diameters.

Moments on circular piles arranged in columns are decreased as compared to moments on an isolated pile. No limits were determined at which the moment became independent of the spacing.

RECOMMENDATIONS

The following experiments on model piles are recommended for comparison purposes with theoretical work and prototype tests.

1. Measurement of wave force distribution on single piles of various diameters are needed in order to compare with Equations (4) and (8).

2. Experiments with a greater number of wave conditions on circular piles, H-sections, flat plates and various other objects are needed in order to establish the relationship of the coefficients of drag and mass to the wave characteristics.

3. Investigation should be made of the mathematical theories pertaining to piles and other objects subject to wave action with respect to force, wave reflection, wave diffraction and flow conditions in the vicinity of the object.

4. Investigation should be made of breaking waves on model structures including the development of force recording equipment.

ACKNOWLEDGMENTS

The above investigations were sponsored by the Office of Naval Research, Bureau of Yards and Docks, The California Company, and International Marine Platforms, Inc.

REFERENCES

Morison, J.R. (1950a) Moment distribution on stepped caisson; Series 35, Issue 1, IER, University of Calif., Berkeley, Calif.

Morison, J.R. (1950b) Moment distribution exerted by waves on piling; Series 35, Issue 2, IER, University of Calif., Berkeley, Calif.

Morison, J.R., (1950c) The forces exerted by waves on marine structures; Series 35, Issue 3, IER, University of Calif., Berkeley, Calif.

Morison, J.R., O'Brien, M.P., Johnson, J.W. and Schaaf, S.A. (1950) The forces exerted by surface waves on piles; Petroleum Trans. AIME, vol. 189, pp. 149-154.

O'Brien, M.P., and Morison, J.R. (1950) The forces exerted by waves on objects; Series 3, Issue 310, IER, University of Calif, Berkeley, Calif.

Snodgrass, F.E., Rice, E.R., and Hall, M. (1951) Wave forces on piling (Monterey field test); Series 35, Issue 4, IER, University of Calif., Berkeley, Calif.

Stokes, Sir G.G. (1901) On the theory of oscillatory waves; Math. and Physical Papers, vol. V, Cambridge University Press

APPENDIX

Corrections to "Design of Piling". Chapter 28, Proceedings of the First Conference on Coastal Engineering;

Page 257, line 13

$$C_M = 2.0 \quad \text{(use theoretical value of 2.0)}$$

Page 257, line 24

$$M_z = \rho \frac{H^2 L^2 D}{T^2} \left\{ \pm C_D K_2 \cos^2\theta + \frac{\pi D}{4 H} K_1 C_M \sin\theta \right\}$$

$$= \frac{(2.0)\ (10)^2\ (452)^2\ (1.5)}{(10)^2} \left\{ +1.6\ (0.0837)(0.9848)^2 \right.$$

$$\left. + \frac{\pi}{4}\ \frac{1.5}{10}\ (0.395)\ (2.0)\ (0.1737) \right\}$$

$$= 612{,}000 \left\{ 0.1294 + 0.0162 \right\} = \underline{\underline{89{,}000 \text{ ft. lbs.}}}$$

Page 258, line 15;

$$M = \rho \frac{H^2\ L^2\ D}{T^2} \left\{ \frac{\pi D}{4 H} K_1 C_M (1) \right\}$$

$$= \frac{(2.0)\ (10)^2\ (452)^2\ (6)}{10^2} \left\{ \frac{\pi}{4}\ \frac{6}{10}\ (0.395)\ (2.0) \right\}$$

$$= \underline{\underline{916{,}000 \text{ ft. lbs.}}}$$